

**NON-INVASIVE IDENTIFICATION OF SYNTHETIC ORGANIC PIGMENTS IN
CONTEMPORARY ART PAINTS BY VISIBLE-EXCITED SPECTROFLUORIMETRY AND
VISIBLE REFLECTANCE SPECTROSCOPY**

M. Longoni, A. Freschi, N. Cicala, S. Bruni*

Dipartimento di Chimica, Università degli Studi di Milano

*Corresponding author

e-mail: silvia.bruni@unimi.it

Dipartimento di Chimica

Università degli Studi di Milano

Via C. Golgi, 19 – 20133 Milano (Italy)

ABSTRACT

The non-destructive, *in-situ* identification of synthetic organic pigments employed in contemporary painting still represents a challenge. In the present study, a non-invasive analytical method based on spectrofluorimetry and visible reflectance spectroscopy was developed to this aim and applied to a considerable number of synthetic organic pigments belonging to the main chemical classes and sold by different manufacturers. In order to discriminate among them, the collected data were processed by a multivariate statistical approach, using principal component analysis (PCA). Moreover, the Kubelka-Munk correction for self-absorption of fluorescence emission was successfully applied to identify pigments in binary mixtures. This approach was finally exploited to recognise the organic pigments used by the artist in a contemporary painting.

KEYWORDS

Synthetic organic pigments, Spectrofluorimetry, Visible reflectance spectroscopy, Contemporary painting

1. INTRODUCTION

Since the discovery of the first synthetic dye, mauveine, by Perkin in 1856, the colouring materials employed by artists have undergone a radical change. In particular, the use of organic synthetic pigments in commercial paints has considerably increased during the 20th century, leading to an expansion of artists' palettes.

Synthetic organic pigments are water-insoluble compounds containing carbocyclic ring systems, often aromatic and sometimes coupled with metal ions. According to their chemical nature, they can be distinguished in different classes: arylide, benzimidazolone, diketo-pyrrolo pyrrole, naphthol, quinacridone, perylene and phthalocyanine are only some examples of the most common ones [1]. Organic pigments span the entire colour range from red to orange, yellow, green, blue and violet depending on their chemical and crystalline structure, and their success is due to excellent physical and chemical properties, such as brightness, heat stability and high tinting strength. All these features made these new colourants really appreciated by contemporary artists, introducing on the other hand a new challenge in the field of diagnostic. In fact, the knowledge of the composition of paints is of great importance for the solution of problems related to the conservation and the restoration of paintings, as well for their valorisation and dating. In addition, many of the early synthetic organic pigments were not particularly lightfast, so their identification can provide information about the degradation and the original appearance of a work of art.

Until now, different analytical techniques have been applied to this purpose, but most of them require sampling. Moreover, identification is often difficult because, thanks to their high tinting strength, synthetic organic pigments are generally present in commercial paints in relatively small amounts and mixed with a considerable volume of other substances, such as binders, fillers and extenders.

In this context, X-ray diffraction (XRD) represents a valuable technique, as in the literature the identification of the chemical and crystalline structure both of pure powder pigments [2] and commercial alkyd and acrylic paints [3] is reported. Also chromatographic methods were successfully used to examine colouring substances: thin layer chromatography (TLC) [4, 5], high-performance liquid chromatography (HPLC) [6] and pyrolysis gas chromatography (pyGC) [7] allowed the identification of a consistent number of pigments, both pure and in commercial paints, and the same goal was achieved by mass spectrometry techniques [7, 8, 9].

However, when working on artistic objects, the importance of non-invasive and *in-situ* applicable analytical methods should be taken into account, but organic pigments represent a challenge precisely in this respect. Being carbon-based compounds, they cannot be analysed by the elemental techniques commonly used *in situ* for the identification of traditional inorganic pigments, such as X-ray fluorescence (XRF). On the other hand, vibrational spectroscopies provide characteristic spectra but,

when applied directly on artistic objects, they are affected by some limitations connected to the presence of binders and additives. Raman spectroscopy was indeed exploited to create a spectral database of organic synthetic pigments [10, 11] but, when analyses are performed directly on works of art, the pigments themselves and/or the binding materials, especially if aged, can cause a huge fluorescence that conceals the weak Raman signals due to the pigments. Even if this limit can be overcome by using new generation handheld Raman spectrometers based on the patented SSETM (Sequentially Shifted Excitation) technology [12], this instrumentation is at present not commonly available in diagnostic laboratories. Fourier-transform infrared (FT-IR) spectroscopy can provide a univocal spectrum, but the presence of binders and fillers often hides with their stronger absorptions the bands of the pigments, making impossible their identification without a preliminary treatment aimed at extracting the colourants and at least partially eliminating the fillers [13].

In this study we evaluated the potentiality for the identification of synthetic organic pigments of two spectrophotometric techniques applicable to paintings *in situ* and in a totally non-invasive way: visible reflectance spectroscopy and visible-excited spectrofluorimetry.

Visible reflectance spectroscopy was already accepted as a common technique in the field of conservation due to its non-destructive nature and easiness of use. However, it is affected by the scarce specificity of the spectral response, characterized by large bands and by absorption maxima obviously similar for pigments of analogous hue [14, 15]. Spectra are also very often characterised by S-shaped and thus even less characteristic patterns, especially for highly concentrated pigments [16]

Spectrofluorimetry, already applied for the *in-situ* identification of natural dyes [15], could instead represent an innovative method for the analysis of modern colouring substances. In fact, the molecules of synthetic organic pigments are rich in multiple bonds and aromatic rings, condition which can promote fluorescence emission, associated with electronic transitions between π orbitals. Therefore, a consistent number of reflectance and fluorescence spectra of the principal organic pigments employed by artists, belonging to the most representative chemical classes and commercialised by different manufacturers, were acquired using a portable spectrophotometer allowing both types of measurements.

In order to consider for identification purposes the entire pattern of the fluorescence and reflectance spectra and not only the wavelength of the emission or absorption maxima, the obtained data were then elaborated through a multivariate approach, based on principal component (PCA) and cluster (CA) analysis, revealing the possibility of recognising a consistent number of organic pigments by combining the information given by the two techniques. Moreover, the Kubelka-Munk correction for self-absorption of fluorescence emission proposed in the literature for paint layers with different

concentration of natural dyes [17, 18] was in this case tested to recognise the components of binary mixtures of pigments of similar or complementary colours.

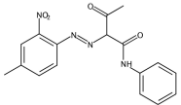
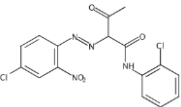
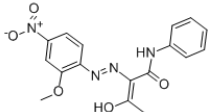
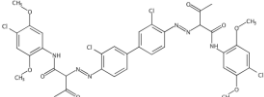
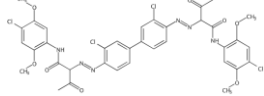
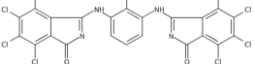
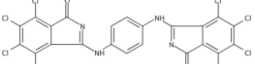
Finally, the approach based on the combination of the two spectrophotometric techniques and multivariate analysis was applied to identify some of the organic pigments used by a contemporary Italian landscape painter, Giuseppe Faraone, in his painting “Addetta a Zoate” (2011).

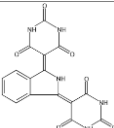
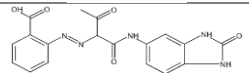
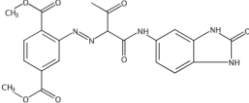
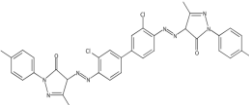
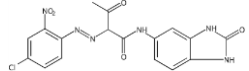
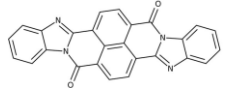
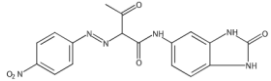
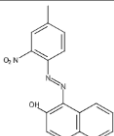
2. MATERIALS AND METHODS

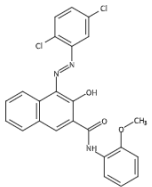
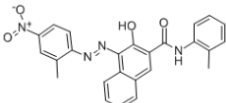
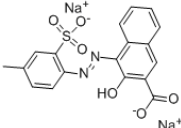
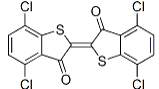
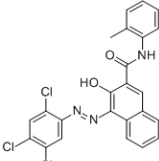
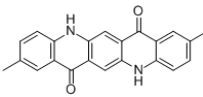
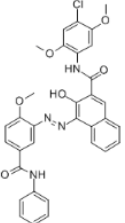
2.1 Reference materials

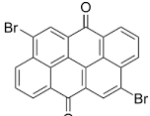
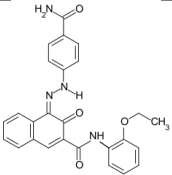
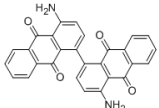
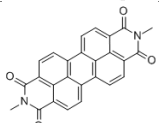
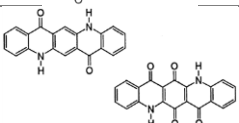
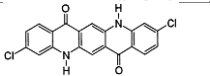
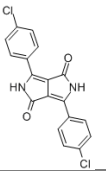
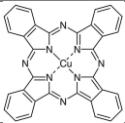
Reference samples of synthetic organic pigments were acquired from some of the main pigment manufacturers. They were pure powders applied on canvas in the laboratory by means of different binders (oil or acrylic) or commercial paints (oil, acrylic or alkyd-based), that were spread on canvas as well. They were chosen in order to consider pigments employed by artists and belonging to the main chemical classes. Moreover, when available, the same pigment was purchased from different manufacturers to compare the corresponding reflectance and fluorescence spectra. Table 1 reports the analysed pigments with their Colour Index (CI) and common name, the chemical class and group, the structural formula, the typology (formulation or powder plus binder) and the manufacturer. **In addition, the inorganic pigments analysed for comparison are listed in the same table.**

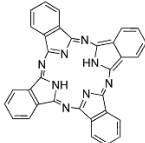
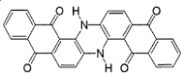
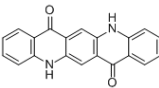
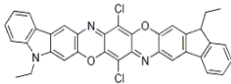
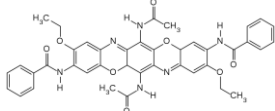
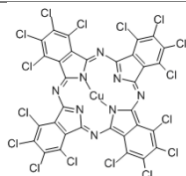
Table 1. Reference pigments analysed in the present work.

CI name	Common name	Chemical class	Chemical group	Structural formula	Typology	Manufacturer
Yellow						
PY1	Hansa yellow G	Monoazo	Acetoacetic arylide		Pure powder	Maimeri
PY3	Hansa yellow 10G	Monoazo	Acetoacetic arylide		Commercial oil Powder Powder Commercial acrylic	Old Holland Classic Oil Kremer Pecchio Maimeri Acrylic
PY35	Cadmium yellow	Inorganic	Cadmium Sulphide	CdS	Powder Commercial oil	Zecchi
PY74	Arylide yellow 5GX	Monoazo	Acetoacetic arylide		Powder	Kremer
PY83	Diarylide yellow HR	Disazo	Diarylide		Powder Commercial acrylic	Maimeri Maimeri Acrylic
PY97	Diarylide yellow FGL	Monoazo	Acetoacetic arylide		Commercial acrylic	Maimeri Brera
PY109	Isoindole yellow	Isoindolinone	Azomethine-type		Powder	Kremer
PY110	Isoindolinone yellow	Isoindolinone	Azomethine-type		Powder	Kremer

PY139	Isoindoline yellow	Isoindoline	Azomethine-type		Powder Commercial alkyd	Maimeri Winsor Griffin
PY151	Benzimidazolone yellow H4G	Monoazo	Benzimidazolone		Powder	Kremer
PY175	Benzimidazolone yellow H6G	Monoazo	Benzimidazolone		Commercial oil	Maimeri Classic Oil
Orange						
PO20	Cadmium orange	Inorganic	Cadmium Selenosulphide	CdS/CdSe	Powder Commercial oil	Zecchi Royal Talens
PO34	Pyrazolone orange	Disazo	Pyrazolone		Commercial acrylic	Maimeri
PO36	Benzimidazolone orange HSL	Monoazo	Benzimidazolone		Powder Commercial acrylic	Maimeri Maimeri Polycolor
PO43	Perinone orange	Polycyclic	Perinone		Powder Commercial oil Commercial acrylic	Maimeri Classic Oil Maimeri Brera Acrylic
PO62	Benzimidazolone orange H5G	Monoazo	Benzimidazolone		Commercial acrylic	Maimeri Polycolor
Red						
PR3	Toluidine red	Monoazo	B-Naphthol		Powder Powder	Kremer Pecchio

PR9	Naphthol AS red	Monoazo	Naphthol-AS		Powder	Kremer
PR12	Permanent bordeaux TRR	Monoazo	Naphthol-AS		Commercial acrylic	Maimeri Polycolor
PR57:1	Lithol rubine	Monoazo	BON lake		Powder	Maimeri
PR88	Thioindigoid violet	Polycyclic	Thioindigo		Powder	Kremer
PR108	Cadmium red	Inorganic	Cadmium Selenide	CdSe	Powder Commercial oil	Zecchi Royal Talens
PR112	Naphthol red AS-D	Monoazo	Naphthol-AS		Powder Commercial acrylic Commercial oil	Kremer Maimeri Old Holland
PR122	Quinacridone magenta	Polycyclic	Quinacridone		Powder	Kremer
PR146	Naphthol red AS	Monoazo	Naphthol-AS		Commercial acrylic	Maimeri

PR168	Anthraquinone scarlet	Polycyclic	Anthraquinone		Commercial acrylic	Maimeri Brera
PR170	Naphthol red AS	Monoazo	Naphthol-AS		Powder	Kremer
PR177	Anthraquinone red	Polycyclic	Anthraquinone		Powder	Kremer
PR179	Perylene maroon	Polycyclic	Perylene&Perino-ne		Powder	Kremer
PR206	Quinacridone burnt scarlet	Polycyclic	Quinacridone		Powder	Maimeri
PR209	Quinacridone red	Polycyclic	Quinacridone		Commercial oil	Maimeri Classic Oil
PR254	Pyrrole red	Polycyclic	Diketopyrrolo-pyrrole		Powder Commercial oil	Maimeri Winsor Griffin
Blue						
PB15:1 PB15:3	Phthalocyanine blue	Polycyclic Polycyclic	Phthalocyanine Phthalocyanine		Acrylic Acrylic	Maimeri Maimeri
PB27	Prussian blue	Inorganic	Ferric Ferricyanide	$\text{Fe}^{\text{III}}_4[\text{Fe}^{\text{II}}(\text{CN})_6]_3$	Powder	Zecchi
PB28	Cobalt blue	Inorganic	Cobalt Aluminate	CoAl_2O_4	Powder	Zecchi

PB29	Ultramarine blue	Inorganic	Complex sulfur-containing sodium-silicate	$(\text{Na,Ca})_8(\text{AlSiO}_4)_6(\text{S,SO}_4,\text{Cl})_{1-2}$	Powder	Zecchi
PB16	Phthalocyanine turquoise	Polycyclic	Phthalocyanine		Powder	Maimeri
PB60	Indanthrone blue	Polycyclic	Antraquinone		Powder	Maimeri
Violet						
PV19	Quinacridone violet	Polycyclic	Quinacridone		Powder Commercial acrylic	Kremer Maimeri
PV23	Dioxazine violet	Polycyclic	Dioxazine		Powder Commercial alkyd	Maimeri Winsor Griffin
PV37	Dioxazine violet	Polycyclic	Dioxazine		Powder	Kremer
Green						
PG7	Phthalocyanine green	Polycyclic	Phthalocyanine		Commercial oil	Maimeri

In the following sections, each pigment will be indicated by its name followed by two letters, the former indicating the binder, the latter the manufacturer as explained in Table 2.

Table 2. Legend of binders and manufacturers.

a	Acrylic
al	Alkyd
o	Oil
P	Acrylic (Primal®)
K	Kremer
M	Maimeri
OH	Old Holland
P	Pecchio
RT	Royal Talens
WG	Winsor&Griffin
Z	Zecchi

2.2 Instrumentation

The analyses were performed using a portable microprobe, suitable for both visible reflectance and fluorescence measurements. The microprobe, equipped with an Olympus 20× objective, is connected by optical fibres to a halogen source (maximum power 150 W) and to a Lot Oriel MS125 spectrometer (grid 400 lines/mm) provided with an Andor CCD detector (1024 × 128 pixel) cooled by means of a Peltier device. The wavelength calibration was based on the emission spectrum of a neon lamp.

The radiation from the source is sent along a direction perpendicular to the microscope objective. For fluorescence analyses the microprobe is thus equipped with an interference filter to select the excitation wavelength and a dichroic filter to eliminate from the spectrum the component due to the exciting radiation. In particular, two different interference filters, centred respectively at 435 nm and 562 nm, were used, while two dichroic filters were available with transmission ranges 458-680 nm and 635-890 nm respectively. Most yellow, orange and red pigments were analysed with excitation at 435 nm, while the wavelength of 562 nm was mainly used to excite the emission of most blue and violet pigments. The fluorescence spectra were collected as sum of 30 scans with an exposure time of 2 seconds and the analyses were preceded by the acquisition of a background spectrum in the absence of the incident radiation.

For visible reflectance analyses the interference filter was removed and the dichroic one was replaced by a beamsplitter 30/70 for the spectral range 400-700 nm. Reflectance spectra were acquired as sum of 30 scans with an exposure time of 0.05 seconds and the analyses were preceded by the acquisition of background and reference spectra. A metal target coated with barium sulphate was used as reference.

2.3 Multivariate analysis of data

Reflectance and fluorescence spectra were processed by principal component analysis (PCA), performed by the statistical package MINITAB 14. The spectra were preliminarily normalised between zero and one to avoid the possible variability due to the reflectance percentage or emission intensity. To perform PCA the covariance matrix was chosen.

2.4 Kubelka-Munk correction for self-absorption of fluorescence emission

In order to consider fluorescence self-absorption and reemission in the solid state, a model based on the Kubelka-Munk theory of diffuse reflectance was applied [17, 18]. According to this model, it is possible to obtain true emission spectra dividing the experimental spectra by a function $\gamma(\lambda, \lambda_0)$, expressed by equation 1:

$$\gamma(\lambda, \lambda_0) = \left(\frac{1}{1 + \sqrt{\frac{\text{Rem}[R(\lambda)]}{\text{Rem}[R(\lambda)] + 2}}} \right)^x \left(\frac{1}{1 + \sqrt{\frac{\text{Rem}[R(\lambda)]\{\text{Rem}[R(\lambda)] + 2\}}{\text{Rem}[R(\lambda_0)]\{\text{Rem}[R(\lambda_0)] + 2\}}} \right) \quad (1)$$

where λ and λ_0 are the emission and excitation wavelength and $\text{Rem}[R(\lambda)]$ is the total remission function defined by the following equation 2:

$$\text{Rem}[R(\lambda)] = \frac{k(\lambda)}{s(\lambda)} = \frac{[1 - R(\lambda)]^2}{2R(\lambda)} \quad (2)$$

where $s(\lambda)$ and $k(\lambda)$ are respectively the scattering and the absorption coefficient and $R(\lambda)$ is the diffuse reflectance at the corresponding wavelength λ .

In this work the self-absorption correction was performed using the GRAMS/AI software.

3. RESULTS AND DISCUSSIONS

3.1 Visible reflectance spectroscopy

All visible reflectance spectra acquired for each pigment and discussed below are reported in Supplementary Material (see Figg. S1-S4)

3.1.1 Red and Orange Pigments

Visible reflectance spectroscopy is generally affected by low specificity for identification purposes and reflectance spectra of pigments having the same colour are very similar, so their identification is challenging. Consequently, PCA analysis (see Fig. S11 in Supplementary Material) allowed us to recognise only few groups in the multivariate space, as almost all red and orange pigments are close to one another. In particular, the identification was possible only for those colorants with a peculiar

hue, for example brown (quinacridone burnt scarlet PR206), or a different shade of red (thioindigoid violet PR88, anthraquinone red PR177, perylene maroon PR179). It is instead difficult when their colour is very similar, as almost all the orange pigments occupy the same region of the score plot, and the same happens for the red ones.

3.1.2 Yellow Pigments

As for the red ones, only few yellow pigments were identifiable by visible reflectance spectroscopy. In particular, PCA (see Fig. S12 in Supplementary Material) allowed us to distinguish in the score plot only two of the colorants analysed: PY109 and PY110, namely isoindole and isoindolinone yellow. Also in this case, this spectroscopic technique suffers indeed from low specificity for the identification of pigments with similar hue.

3.1.3 Violet and Blue Pigments

Among the pigments analysed, PV19 belongs to the quinacridone family and is characterised by a pink-reddish hue; PV23 and PV37 are member of the dioxazine group and their colour has a blue shade. For this reason, the former was considered together with red and orange pigments (section 3.1.1), while the latter were analysed separately together with blue ones. It is worth noting that PV19 formed two different groups, one corresponding to the pure pigment purchased from Kremer and mixed with different binders and the other corresponding to the commercial acrylic paint sold by Maimeri. This dual behaviour is due to the fact that the two pigments are two different crystalline phases of quinacridone [19, 20], respectively β for Maimeri and γ for Kremer, as confirmed by XRD analyses (see Fig. S14 in Supplementary Material). The γ -phase is characterised by a bluish shade, the β one is instead reddish, explaining their different reflectance spectra.

The score plot of the PCA (Fig. 1) performed on violet and blue pigments revealed the impossibility of distinguishing the dioxazine violets PV23 and PV37, whose colour is very similar. The inorganic pigments cobalt blue (PB28) and ultramarine blue (PB29) are well recognisable, while Prussian blue (PB27) is located close to the indanthrone and phthalocyanine blue PB60 and PB16, which cannot be distinguished from their reflectance spectra. Finally, the two crystalline phases of Phthalocyanine Blue PB15, PB15:1 and PB15:3, occupy two different areas in the centre of the score plot. This is due to the fact that the two forms of copper phthalocyanine, alpha and beta respectively, have different chromatic shade, reddish-blue for the former and greenish for the latter. [21]

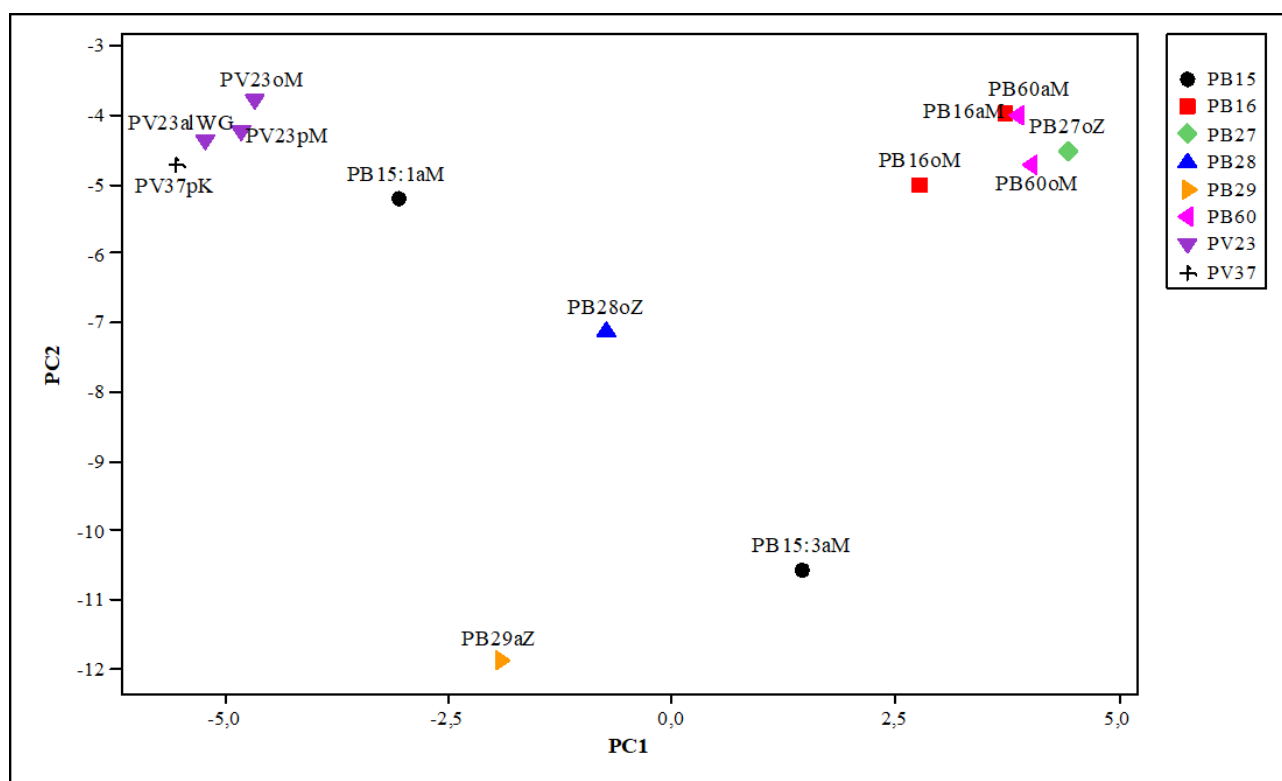


Fig. 1. Score plot of the first two principal components of the visible reflectance spectra of violet and blue pigments in painting mock-up samples on canvas.

3.2 Spectrofluorimetry

Most of the analysed pigments showed fluorescence emission, more or less intense according to their chemical structure. The corresponding spectra are reported as Supplementary Material (see Fig. S5-S7). Only a limited number of pigments resulted to be not fluorescent, namely PR170 (naphthol red AS), PR177 (anthraquinone red), PR179 (perylene maroon), PR88 (thioindigoid violet) and PR206 (quinacridone burnt scarlet). On the other hand, it is worth noting that three of them, namely PR206, PR179 and PR88, are between the few pigments recognisable from their reflectance spectrum.

In the following sections, multivariate analysis performed on red, orange and yellow fluorescent pigments will be presented. Given their smaller number, blue and violet pigments were instead compared just on the basis of their spectral pattern.

3.2.1 Red and orange Pigments

PCA analysis allowed us to verify that almost all paint samples of the same pigment are located in the same region of the score plot (Fig. 2), forming an independent group regardless of the manufacturer and the binders employed. In particular, PR3 (toluidine red), PR12 (permanent

bordeaux TRR), PR122 (quinacridone magenta), PR146 (naphthol red AS), PR168 (anthraquinone scarlet), PR209 (quinacridone red), PR254 (pyrrole red), PO34 (pyrazolone orange), PO36 (benzimidazolone orange HSL), PO43 (perinone orange) and PO62 (benzimidazolone orange H5G) were discernible, while some overlapping was observed for the paint samples of a few other pigments, as detailed below. Quinacridone violet PV19 formed again two different groups in the score plot, each corresponding to a different crystalline phase. The γ -phase of PV19 (Kremer) has a fluorescence emission similar to PR57:1 (lithol rubine), but, being of two different colours, we can discriminate these pigments from their reflectance spectra (section 3.1.1). The β -phase (Maimeri) corresponds to a well-defined group in the score plot. Finally, PR9 (naphthol AS red) is located close to PR112 (naphthol red AS-D) and PR146 (naphthol red AS), but this can be explained by the fact that their chemical structures are similar, as they all belong to the class of Naphthol AS red pigments. The emission maxima of the pigments are summarised in Fig. 3.

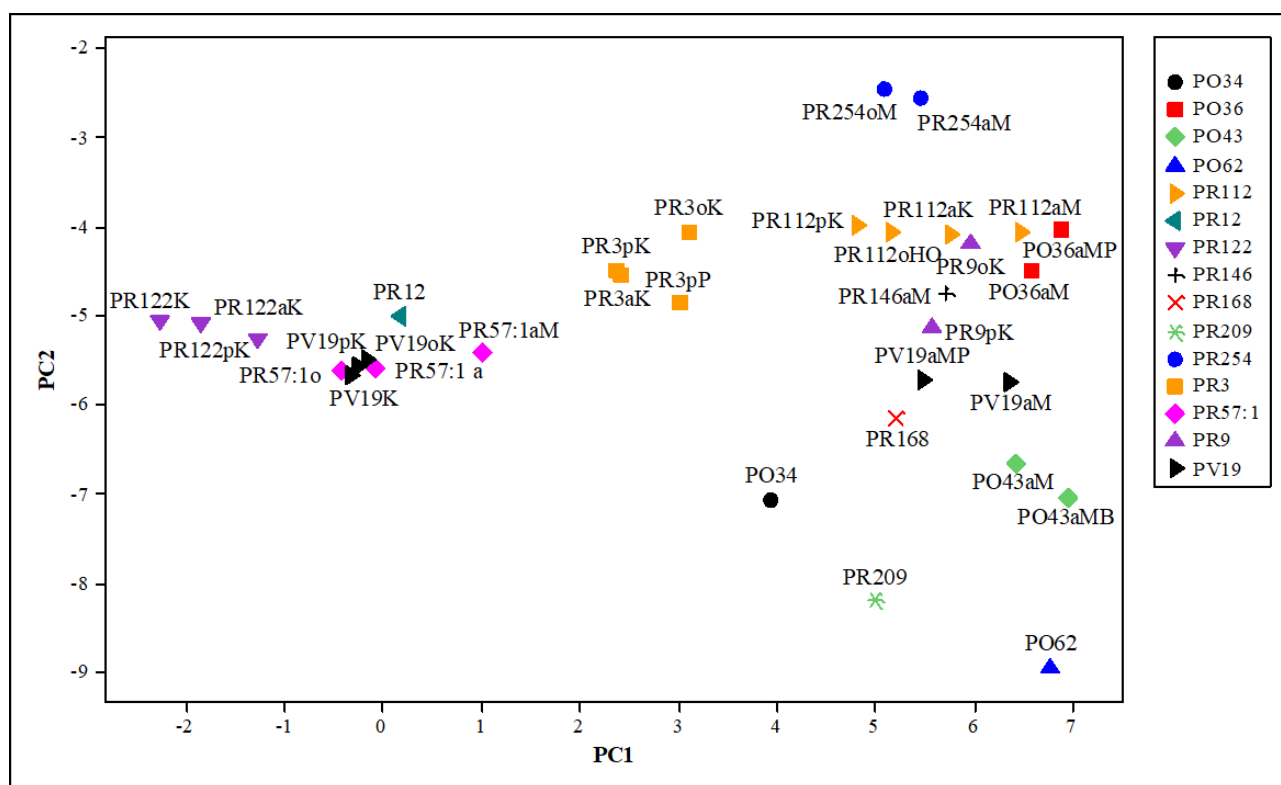


Fig. 2. Score plot of the first two principal components of the emission spectra ($\lambda_{exc} = 435$ nm) of red and orange pigments in painting mock-up samples on canvas.

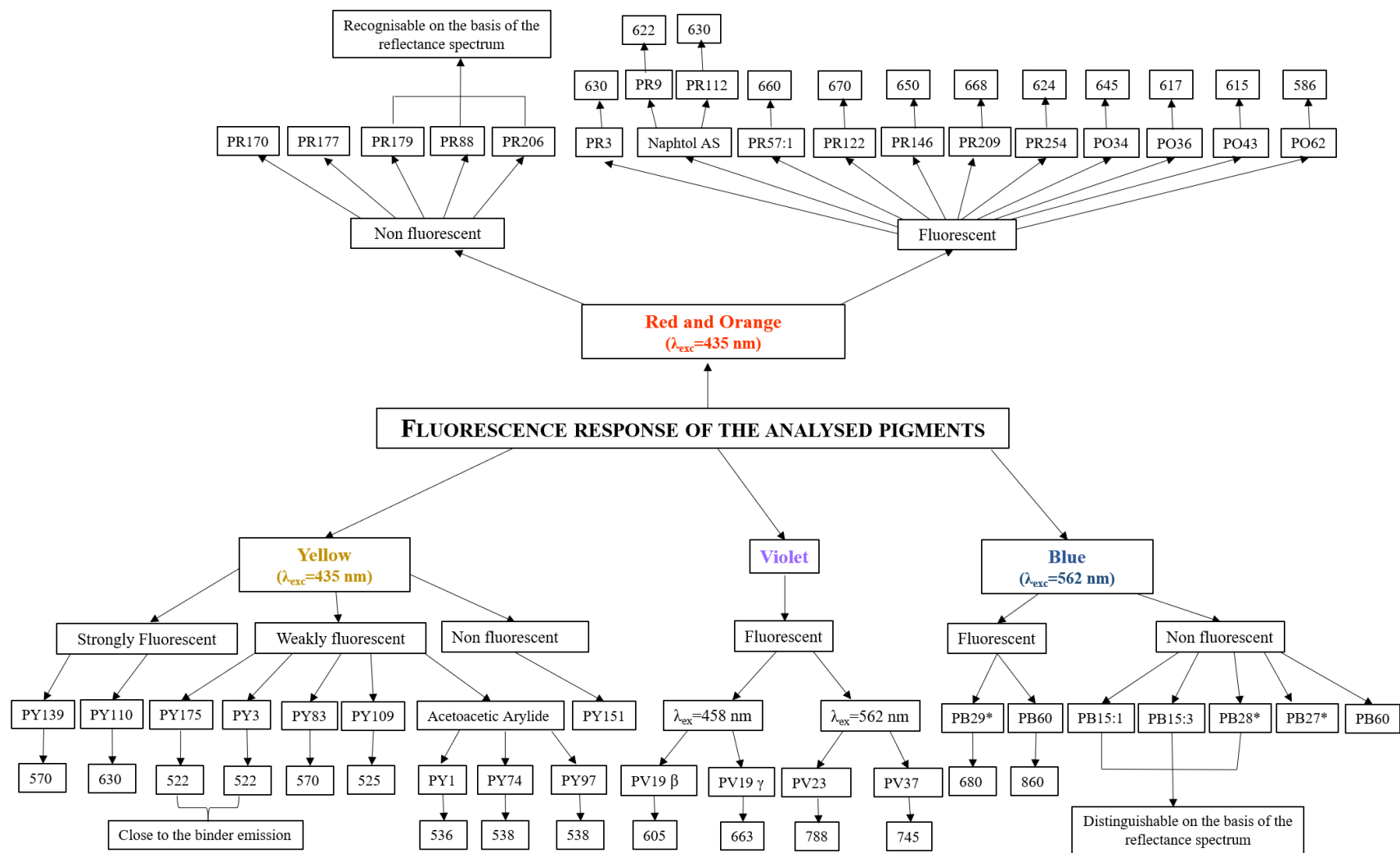


Fig. 3. Scheme of the fluorescence response of the pigments examined in the present work. The wavelength of emission maxima is expressed in nanometres (nm).

* = blue inorganic pigments.

3.2.2 Yellow Pigments

Fluorescence emission of yellow pigments is generally close to that of pure binders (acrylic or oil), which give a spectrum characterised by a maximum around 520 nm (see Fig. S8 in Supplementary Material). The emission due to the binders can thus hide that of the pigments, making more complex and sometimes preventing their identification. An exception is represented by PY139 (isoindoline yellow) and PY83 (diarylide yellow HR), that in the score plot occupy a region well separated from all other yellow pigments (see Fig. S13 in Supplementary Material). In fact, both their spectra show a maximum at 570 nm, but on the other end they can be easily distinguished considering that PY139 has a very intense fluorescence emission in contrast to PY83, whose signal is significantly weaker. PCA analysis was thus repeated excluding PY139 and PY83, in order to obtain a score plot where the different groups formed by the other yellow pigments could be more easily recognised (Fig. 4). The Hansa yellow 10G (PY3) group is close to the binder group and indeed this pigment, as well as benzimidazolone yellow PY175, is only weakly fluorescent. This is especially true for the commercial formulations of PY3, in comparison with the painting samples obtained in the laboratory by mixing the pure pigment and the binders. Most probably, the pigment concentration in the industrial products is lower because of the presence of fillers and additives, which further decrease its already weak fluorescence.

In the lower left part of the score plot, three pigments are located, namely PY1 (Hansa yellow G), PY74 (arylide yellow 5GX) and PY97 (arylide yellow FGL), all belonging to the same chemical family (monoazo) and group (acetoacetarylide).

The isoindole yellow PY109 showed a weak fluorescence signal, with a low signal/noise ratio, justifying the random position of the corresponding painting samples in the multivariate hyperspace; anyway, its identification can be confirmed on the basis of its reflectance spectrum (section 3.1.2).

Finally, isoindolinone yellow PY110, which was not included in this PCA, is well identifiable from its fluorescence emission because it is the one yellow pigment giving an emission maximum around 635 nm.

In conclusion, PCA analysis revealed that it is difficult to distinguish all the different yellow pigments, because their fluorescence emission is often weak and overlapped the one of binders. In any case, the multivariate approach allowed us to discriminate pigments belonging to the same chemical classes whose fluorescence emission is indeed similar. The emission maxima of these pigments are summarised in Fig. 3.

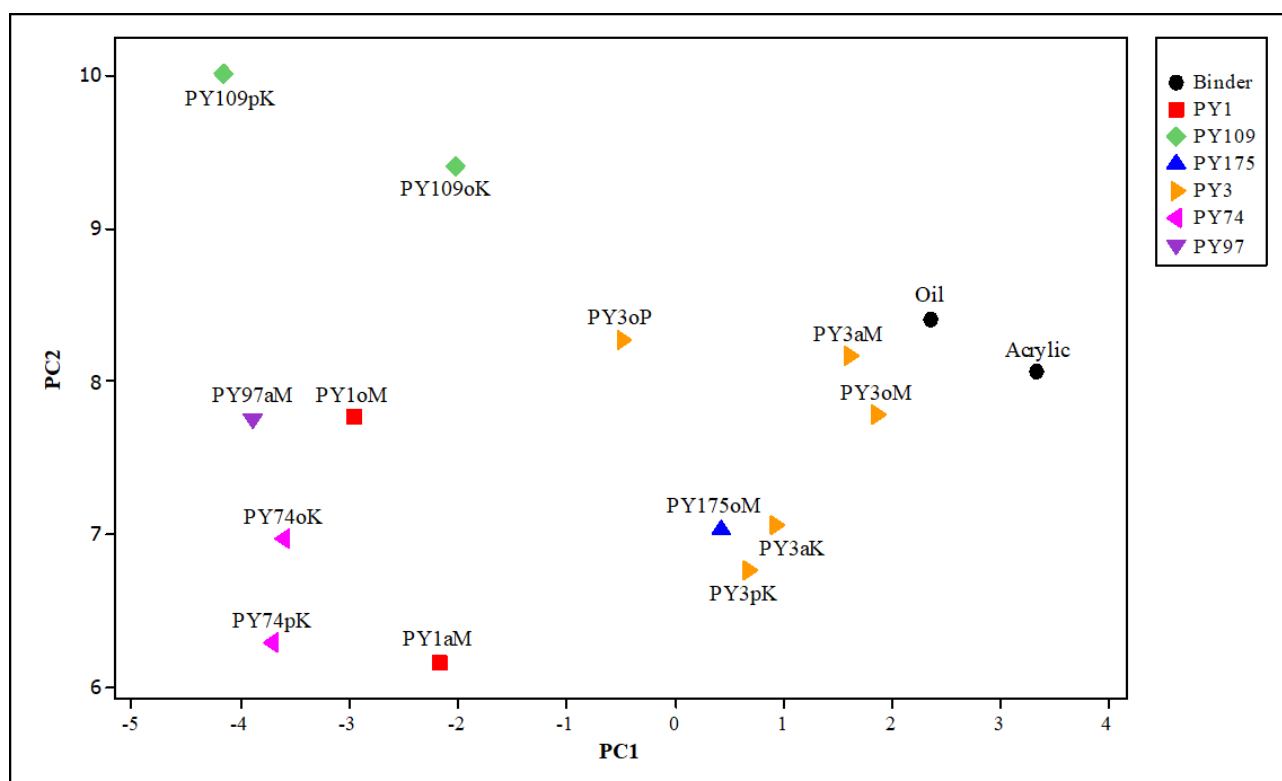


Fig. 4. Score plot of the first two principal components of the emission spectra ($\lambda_{exc} = 435$ nm) of yellow pigments with fluorescence maxima between 520 and 540 nm (spectra obtained from painting mock-up samples on canvas).

3.2.3 Violet Pigments

All the violet pigments here analysed resulted to be fluorescent. **Quinacridone violet** PV19 showed a fluorescence emission when excited at 435 nm, therefore its spectrum was considered together with those of red and orange pigments (section 3.2.1). **The two dioxazine violets** PV23 and PV37 are not fluorescent if excited at this wavelength, but they revealed characteristic emission bands (Fig. 5) that allowed us their identification when excited at 562 nm. In particular, an emission maximum was observed around 743 nm for PV23 and at 786 nm for PV37. Given the limited number of pigments with such a hue, no multivariate analysis was performed on the corresponding spectral data. However, spectrofluorimetry demonstrated to be a powerful technique to distinguish PV23 and PV37, whose identification is not possible if only based on visible reflectance spectra. The emission maxima of these pigments are summarised in Fig. 3.

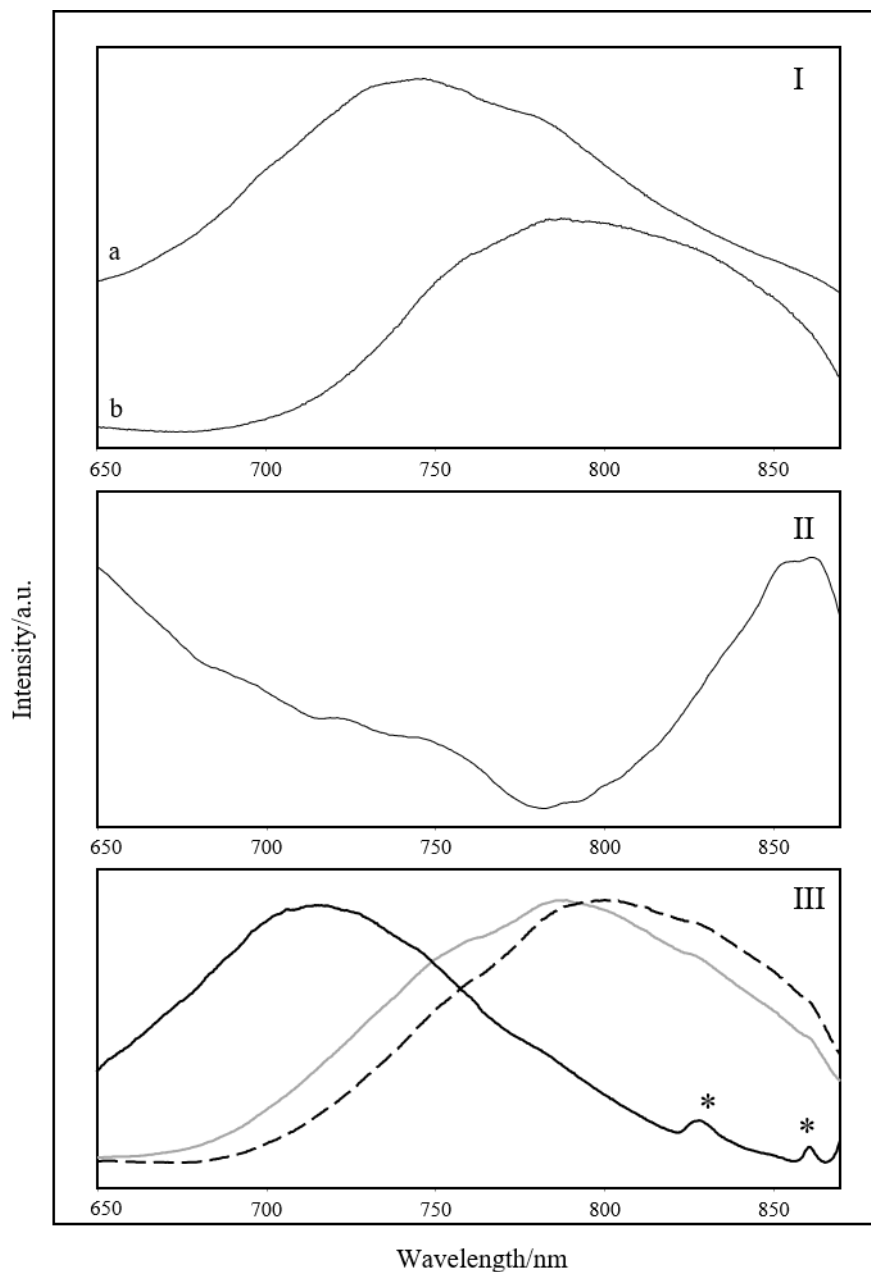


Fig. 5. (I) emission spectra ($\lambda_{\text{exc}} = 562 \text{ nm}$) of the two dioxazine violets PV23 (a) and PV37 (b) in painting mock-up samples on canvas (commercial alkyd and powder plus oil respectively); (II) emission spectra ($\lambda_{\text{exc}} = 562 \text{ nm}$) of PB16 in painting mock-up samples on canvas (powder plus oil); (III) emission spectra ($\lambda_{\text{exc}} = 435 \text{ nm}$) of cadmium yellow PY35 (black line), orange PO20 (grey line) and red PR108 (dashed line) in painting mock-up samples on canvas (powder plus oil). *= spurious band due to the dichroic filter.

3.2.4 Blue Pigments

Among the three blue organic pigments analysed, only PB16 (phthalocyanine blue) exhibited fluorescence emission upon excitation at 562 nm. In fact, this pigment, which is chemically a phthalocyanine, has an emission band around 850 nm (Fig. 5).

PB15 is a phthalocyanine too, but it is not fluorescent, presumably due to the presence, in the centre of the porphyrin ring, of the paramagnetic copper(II) ion that quenches the emission. Both crystalline phases of such pigment, PB15:1 and PB15:3, showed the same behaviour, but they can be recognised on the basis of their reflectance spectra (section 3.2.3, [22])

PB60 belongs instead to a different chemical class, being an anthraquinonic compound, and it did not show any fluorescence emission upon excitation at 562 nm. Anyway, its reflectance spectrum is different from those of PB15 making possible the distinction between these two non-fluorescent organic blue pigments, even if it is quite similar to that of the inorganic **Prussian blue** PB27. The results are summarised in Fig. 3.

Moreover, spectrofluorimetry was proved suitable to recognise also one of the most important - in the past and nowadays- inorganic pigments, **ultramarine blue** (PB29), thanks to a fluorescence band whose maximum is around 680 nm. A similar orange fluorescence emission has already been observed in alkali glasses containing sulphur [23, 24], which have an analogous composition to this pigment.

3.2.5 Inorganic cadmium-based pigments

Besides organic pigments, spectrofluorimetry can be exploited to identify cadmium-based pigments as already suggested by De la Rie [25]. Cadmium yellow, orange and red are composed of cadmium sulphide (CdS) or cadmium selenium sulphide (CdS/CdSe). In the pure crystal form, they are not fluorescent, but the presence of a very small amount of impurities can cause under UV light a fluorescence emission in the red and infrared region of the electromagnetic spectrum. From yellow to red, a shift of the band towards longer wavelengths is observed (Fig. 5 and [25]). In the present study we demonstrated the possibility of exciting the fluorescence of cadmium-based pigments also employing visible radiation at 435 nm. Therefore, the interference filter centred at 435 nm was coupled with the dichroic one at 635 nm in order to collect the emission response in the 600-900 nm spectral range.

The presence of these fluorescence bands was confirmed by analysing both pure powder pigments as such and mixed with binders and commercial paints (see Fig. S10 in Supplementary Material).

3.2.6 Self-absorption correction applied to mixtures of pigments

The self-absorption correction described in section 2.4 was in the present work applied to binary mixtures: when two pigments are mixed together, the fluorescence spectrum is affected by the presence of both colouring substances. In particular, an apparent shift of the fluorescence band caused by the absorption due to the second component and a changing in fluorescence intensity can occur.

Therefore, we investigated the possibility of identifying each component applying the self-absorption correction. For this purpose, three different kind of mixtures were prepared by mixing two commercial acrylic paints and analysed:

- (a) Two fluorescent pigments with fluorescence emission of comparable intensity: PY139+PR122 (1:1)
- (b) Two fluorescent pigments having complementary colours: PY139+PV23 (2:1)
- (c) A fluorescent and a weakly fluorescent pigment: PR112 +PY3 (1:1)

Their reflectance and fluorescence spectra were acquired and the correction was performed. In order to investigate the possibility of recognising the two pigments forming each mixture, the corrected spectra were compared to those of the pure components, corrected as well for their self-absorption.

In case (a), the uncorrected spectrum showed a fluorescence band around 625 nm, corresponding to that of pure **quinacridone magenta** PR122. After the self-absorption correction, a broad band with two maxima appeared: the former is referable to **isoindoline yellow** PY139 (570 and 540 nm), the latter corresponds to the corrected spectrum of PR122 (614 nm). Therefore, the correction allowed us to identify the two fluorescent components of the mixture (Fig. 6).

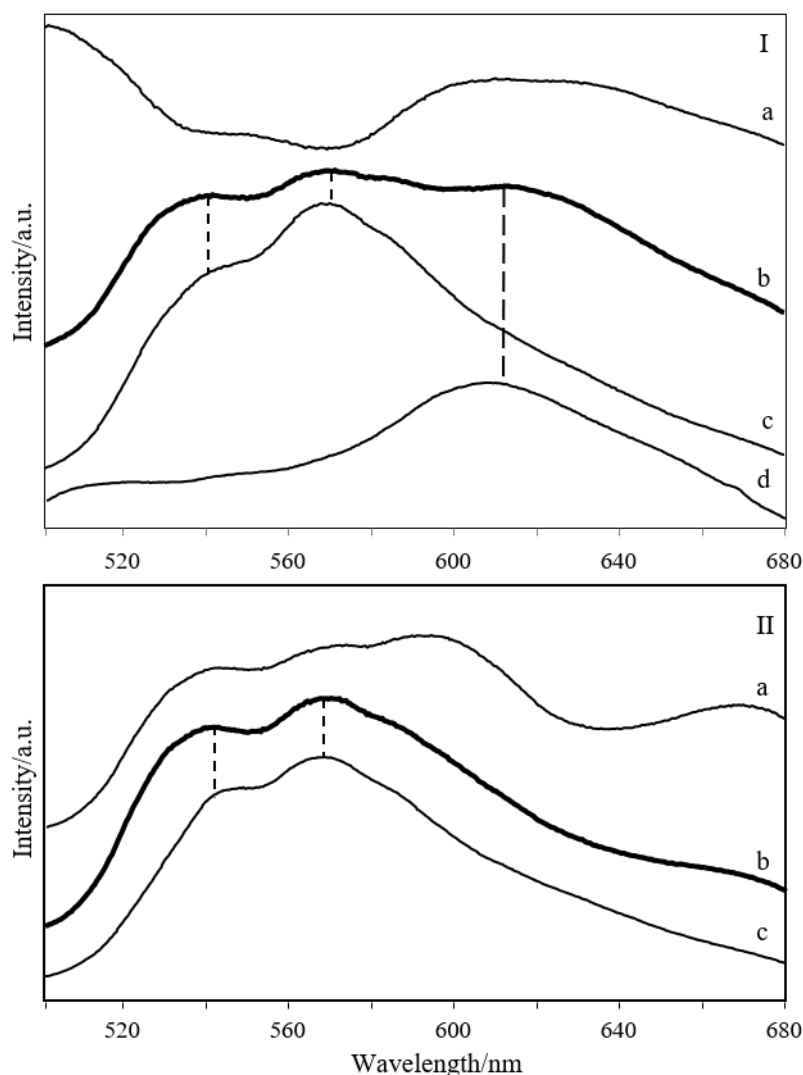


Fig. 6. (I) Emission spectra of a painting sample with acrylic binder of the mixture PY139+PR122 ($\lambda_{\text{exc}} = 435$ nm), before (a) and after (b) correction for self-absorption. For comparison, also the corrected spectra of the two pigments (c, d) are shown; (II) Emission spectra of a painting sample with acrylic binder of the mixture PY139+PV23 ($\lambda_{\text{exc}} = 435$ nm), before (a) and after (b) correction for self-absorption. For comparison, also the corrected spectrum of PY139 is shown (c).

In case (b), the analyses were performed with the two different filter combination (interference 435 nm/dichroic 458 nm and interference 562 nm/dichroic 635 nm) in order to verify if, exciting separately the fluorescence of the two complementary pigments, their identification in mixture is still possible. At $\lambda_{\text{exc}} = 435$ nm, before the correction, the spectrum is characterised by two fluorescence bands (at 591 nm with two shoulders at 541 and 570 nm and at 668 nm) and apparently it is not attributable to any pigment. Once corrected, a single band at 568 nm with a shoulder at 540 nm appears and the spectrum becomes very similar to that of pure **isoindoline yellow** PY139, allowing

us the identification of this component (Fig. 6). At $\lambda_{\text{exc}} = 562$ nm, a spectrum characterised by a weak band is obtained. After the self-absorption correction, it shifts towards shorter wavelengths, but the identification of PV23 (dioxazine violet) is still impossible, probably due to the dilution of the pigment in the mixture.

In case (c), the emission spectrum allowed us to recognise the fluorescent pigment PR112 (naphthol red AS-D) in mixture with the weakly fluorescent pigment PY3 (Hansa yellow 10G) and the self-absorption correction worked as in the case of paint layers of different concentration [17]. In the solid state, a re-absorption of the emitted radiation by molecules of the same compound can occur, causing a quenching of the fluorescence and a shift of the band towards longer wavelengths. These phenomena are related to the concentration of the pigment: increasing the concentration results in a reduction of the emission intensity and in a red shift of the emission maximum. Therefore, the emission spectrum of PR112 in mixture with PY3 is not immediately comparable with that of the pure reference pigment due to the different concentration. The correction for self-absorption shifted the emission maximum towards lower wavelengths, making the spectrum of the fluorescent pigment diluted in the mixture more similar to that of the pure one corrected as well (see Fig. S9 in Supplementary Material). It is worth noting that the corresponding reflectance spectrum, which exhibits an edge at an intermediate wavelength between those of the two pure pigments, is of less use in identifying this component.

3.3 Case study

The methodology applied to the identification of reference pigments was extended to a real painting. The object under investigation was “Addetta a Zoate”, an oil panel painted by G. Faraone in 2011. During a previous campaign of scientific examinations [12], Raman analyses were carried out allowing us the identification of the pigments employed by the artist. In the present study, the analytical approach based on visible reflectance spectroscopy and spectrofluorimetry was performed in order to confirm its potentiality. For this purpose, areas of different colours were examined and their spectra were compared to those of the reference pigments in order to identify the colorants employed (Fig. 7).

Green: In dark green areas corresponding to the trees in the background (point 5), the reflectance spectrum (see Fig. S15 in Supplementary Material) allowed us to recognise the pigment phthalocyanine green PG7, which is not fluorescent. Moreover, the emission spectra obtained exciting at 435 nm and collecting the emission response in the range 600-900 nm demonstrated the use of cadmium yellow (PY35) to lighten the colours in the light green details, such as grass (point 4) and

willows (point 6). This information was only achieved by spectrofluorimetry, as the reflectance spectrum is dominated by the response of the green pigment.

Red: The red colour is present in few details of the painting, namely some small flowers (point 2) and the artist's signature (point 1). Upon excitation at 435 nm, an emission band with maximum at 597 nm was observed. However, no correspondence was found with any of the red or orange pigments examined in the present work. Indeed, previous analyses [12] demonstrated the use of a benzimidazolone pigment, possibly PO60, that however was not available to us for comparison. Indeed, the benzimidazolone orange pigment analysed in the present work, PO36, shows an emission maximum at a higher wavelength. Finally, the possible presence of a cadmium pigment was ruled out due to the colour of the NIR emission band.

Pink: The pink colour used by the artist to paint the clouds (point 3) was probably a mixture between an orange and a white pigment. The corresponding pigment could be identified upon comparing its emission spectrum corrected for self-absorption with the spectrum of reference perinone orange PO43 (main band at 615 nm) corrected as well (see for comparison mixture (c) discussed above). In this way the effect of the remarkably different concentration of the pigment in the light-coloured detail of the painting and in the reference mock-up sample was taken into account. Raman analyses confirmed the use of the perinone orange pigment [12].

Violet: In violet areas dioxazine violet PV23 was recognised. In particular, the violet flowers (point 8) were painted using this pure pigment, while in the violet brush strokes on the trees (point 7) it seems to be mixed with ultramarine blue (PB29), as the growing trend of the fluorescence spectrum around 650 nm suggests. The results achieved were confirmed by supplementary Raman analyses.

Blue: PCA did not allow us to recognise the blue pigments (point 9) in the paintings starting from their reflectance spectra. Upon excitation at 562 nm, fluorescence analyses revealed instead the presence of PB29, the ultramarine blue. The previous Raman analyses confirmed the use of this pigment mixed with PB15:3 (phthalocyanine blue), which is not detectable by spectrofluorimetry.

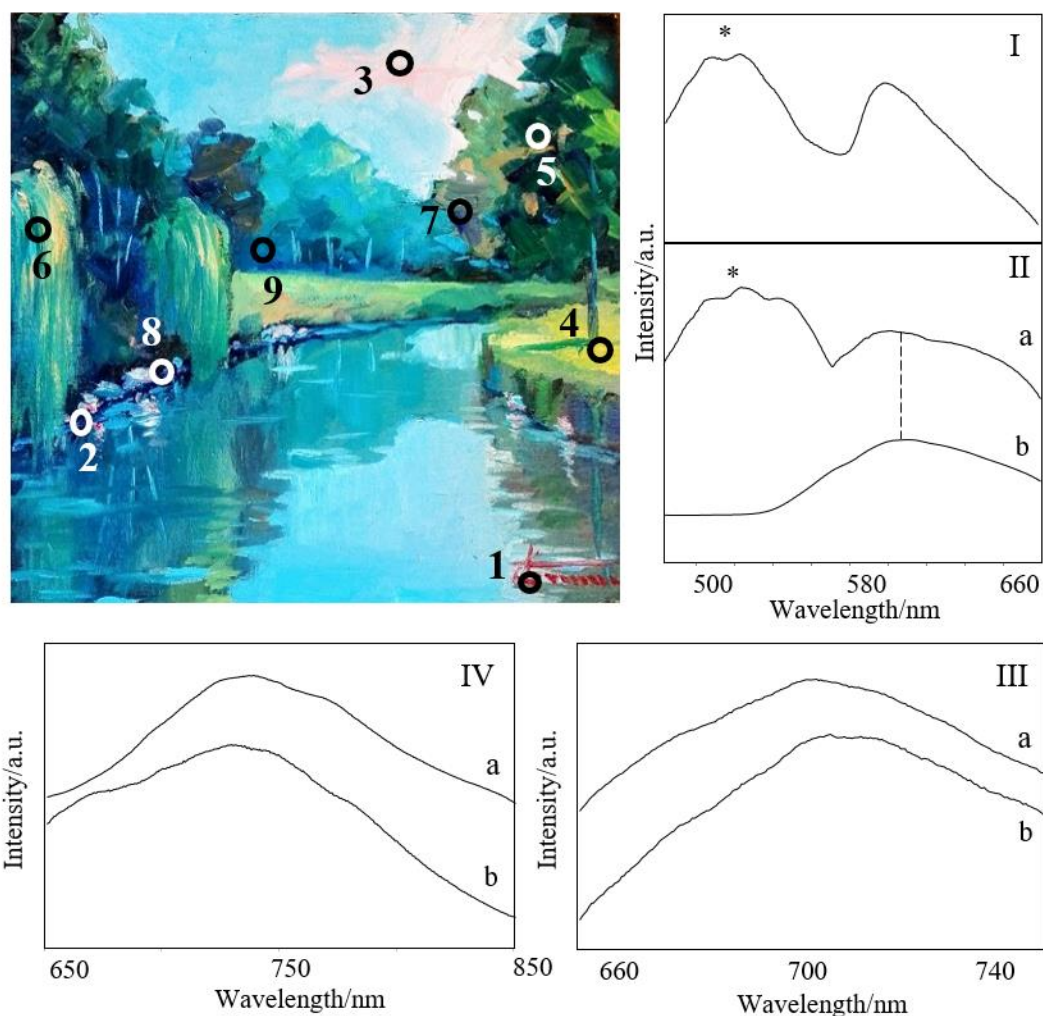


Fig. 7. Measurement areas and emission spectra obtained on the painting “Addetta a Zoate” (G. Faraone, 2011). (I) emission spectrum ($\lambda_{\text{exc}} = 435 \text{ nm}$) of point 1 (red); (II) emission spectrum ($\lambda_{\text{exc}} = 435 \text{ nm}$) of (a) point 3 (pink) after self-absorption correction, compared with that of the recognised reference pigments PO43 (b); (III) emission spectrum ($\lambda_{\text{exc}} = 435 \text{ nm}$) of (a) PY35 compared with that of (b) point 4 (light green); (IV) emission spectrum ($\lambda_{\text{exc}} = 562 \text{ nm}$) of (a) PV23 compared with that of (b) point 7 (violet). * = band due to oil binder.

4. CONCLUSIONS

By combining visible-excited spectrofluorimetry and visible reflectance spectroscopy it was possible to recognise a significant number of synthetic organic pigments, representing the colouring matter in contemporary artists' paints.

Most red, orange and yellow pigments turned out to exhibit an appreciable fluorescence emission upon visible excitation, allowing us to identify them, or at least the chemical class to which they belong. Almost all the non-fluorescent ones could be instead identified through their visible

reflectance spectrum. Cadmium pigments, examined for comparison, were recognisable thanks to a characteristic fluorescence band around 800 nm.

Among the blue pigments, only PB16 resulted to be fluorescent, but upon combining the information given by spectrofluorimetry and PCA applied to reflectance spectra their identification was still possible.

Finally, all the examined violet pigments were fluorescent and could be identified on the basis of the different wavelengths of their emission maxima.

Moreover, the Kubelka-Munk correction of emission spectra for self-absorption was successfully applied to recognise fluorescent pigments in binary mixtures.

This method was finally tested on a real painting, leading to the identification of the pigments (pure or in mixtures) employed by the artist.

In summary, the use of spectrofluorimetry, possibly integrated by that of visible reflectance spectroscopy and combined with multivariate analysis of spectral data, proved quite efficient for the identification of synthetic pigments, in spite of the broad bands that usually characterize electronic spectra. The main advantage of the present method lies of course in the possibility of applying it in a non-invasive manner and “in situ” by means of portable instrumentation, thus obtaining complementary information to that supplied by other non-destructive techniques.

ACKNOWLEDGEMENTS

The authors wish to thank Mr. Amatore Marchesi of Industria Maimeri Spa (Italy) for kindly supplying several pigments used in the formulation of Maimeri artists' paints.

REFERENCES

- [1] Lomax, S.Q., Learner T., A Review of the Classes, Structures, and Methods of Analysis of Synthetic Organic Pigments, *J. Am. Inst. Conservat.*, 45 (2) (2006), 107-125.
- [2] Lomax S.Q., The application of X-ray powder diffraction for the analysis of synthetic organic pigments. Part 1: dry pigments, *J. Coat. Technol. Res.*, 7 (3) (2010), 331-346.
- [3] Lomax S.Q., The application of X-ray powder diffraction for the analysis of synthetic organic pigments. Part 2: artists paint, *J. Coat. Technol. Res.*, 7 (3) (2010), 325-330.
- [4] Milovanovic G.A., Ristic-Solajic M., Janjic T.J., Pigments in artists' paints by thin-layer chromatography, *J. Chromatogr.*, 249 (1982), 149-154.
- [5] Massonnet G., Stoecklein W., Identification of organic pigments in coatings: application to red automotive topcoats. Part I: Thin layer chromatography with direct visible microspectrophotometric detection, *Sci. Justice*, 39 (2) (1999), 128-134.
- [6] Wegener J.W., Klamer J.C., Govers H., Brinkman U.A., The determination of organic colourants in cosmetic products by High-performance Liquid Chromatography, *Chromatographia*, 24 (1987), 865-875.
- [7] Russell J., Singer B.W., Perry J.J., Bacon A., The identification of synthetic organic pigments in modern paints and modern paintings using pyrolysis-gas chromatography–mass spectrometry, *Anal. Bioanal. Chem.*, 400 (2011), 1473-1491.
- [8] Kirby D.P., Khandekar N., Sutherland K., Price B.A., Application of laser desorption mass spectrometry for the study of synthetic organic pigments in works of art, *Int. J. Mass Spectrom.*, 284 (2009), 115-122.
- [9] Menke C.A., Rivenc R., Learner T., The use of direct temperature-resolved mass spectrometry (DTMS) in the detection of organic pigments found in acrylic paints used by Sam Francis, *Int. J. Mass Spectrom.*, 284 (2009), 2-11.
- [10] Scherrer N.C., Zumbuehl S., Delavy F., Fritsch A., Kuehnen R., Synthetic organic pigments of the 20th and 21st century relevant to artist's paints: Raman spectra reference collection, *Spectrochim. Acta, Part A*, 73 (2009), 505-524.
- [11] Fremout W., Saverwyns S., Identification of synthetic organic pigments: the role of a comprehensive digital Raman spectral library, *J. Raman Spectrosc.*, 43 (2012), 1536-1544.
- [12] Bruni S., Guglielmi V., Raman Spectroscopy for the Identification of Materials in Contemporary Painting, in Vandenabeele P., Edwards H. (eds.), *Raman Spectroscopy in Archaeology and Art History (Vol.2)*, The Royal Society of Chemistry, 2019, p.168.
- [13] Jonsson J., Learner T., Separation of acrylic paint components and their identification with FTIR spectroscopy. Proceedings of the 6th Infrared and Raman Users Group (IRUG 6). Ed. M. Picollo. Florence: Il Prato, 58-63. 2004.

- [14] Gulmini M., Idone A., Diana E., Gastaldi D., Vaudan D., Aceto M., Identification of dyestuffs in historical textiles: strong and weak points of a non-invasive approach, *Dyes Pigm.*, 2013, 98, 136-145.
- [15] Zaffino C., Bertagna M., Guglielmi V., Dozzi M.V., Bruni S., In-situ spectrofluorimetric identification of natural red dyestuffs in ancient tapestries, *Microchem. J.*, 139 (2018), 77-82.
- [16] M. Bacci, "UV-VIS-NIR, FT-IR, and FORS spectroscopies, in Ciliberto E., Spoto G. (eds.) *Modern Analytical Methods in Art and Archaeology*, J. Wiley & Sons, New York, 2000, p. 343.
- [17] Clementi C., Miliani C., Verri G., Brunetti B.G., Sgamellotti A., Application of the Kubelka-Munk correction for self-absorption of fluorescence emission in carmine lake paint layers., *Appl. Spectrosc.*, 63 (12) (2009), 1323-1330.
- [18] Verri G., Clementi C., Comelli D., Cather S., Piqué F., Correction of ultraviolet-induced fluorescence spectra for the examination of polychromy, *Appl. Spectrosc.*, 62 (12) (2008), 1295-1302.
- [19] Paulus E.F., Leusen F.J.J., Schmidt M.U., Crystal structures of quinacridones, *CrystEngComm*, 9 (2007), 131-143.
- [20] Binant C., Guineau B., Lautié A., The application of electronic and vibrational spectroscopic techniques to the identification of quinacridone pigments in vehicle paint systems, *J. Soc. Dyers Colour.*, 106 (1990), 187-191
- [21] <https://www.handprint.com/HP/WCL/pigmt1d.html>
- [22] Poldi G., Caglio S., Phthalocyanine identification in paintings by reflectance spectroscopy. A laboratory and in situ study, *Opt. Spectrosc*, 114 (2013), 929–935.
- [23] Paul A., Ward A., Gomolka S., Origin of the blue colour in alkali-borate glasses containing sulphur, *J. Mater. Sci.*, 9 (1974), 1133-1138.
- [24] Giggenbach W., The blue solutions of sulphur salt melts, *Inorg. Chem.*, 10 (6) (1971), 1308-1311.
- [25] Rene de la Rie E., Fluorescence of Paint and Varnish Layers (Part I), *Stud. Conserv.*, 27 (1982), 1-7.

FIGURE CAPTIONS

Fig. 1. Score plot of the first two principal components of the visible reflectance spectra of violet and blue pigments in painting mock-up samples on canvas.

Fig. 2. Score plot of the first two principal components of the emission spectra ($\lambda_{\text{exc}} = 435$ nm) of red and orange pigments in painting mock-up samples on canvas.

Fig. 3. Scheme of the fluorescence response of the pigments examined in the present work. The wavelength of emission maxima is expressed in nanometres (nm). * = blue inorganic pigments.

Fig. 4. Score plot of the first two principal components of the emission spectra ($\lambda_{\text{exc}} = 435$ nm) of yellow pigments with fluorescence maxima between 520 and 540 nm (spectra obtained from painting mock-up samples on canvas).

Fig. 5. (I) emission spectra ($\lambda_{\text{exc}} = 562$ nm) of PV23 (a) and PV37 (b) in painting mock-up samples on canvas (commercial alkyd and powder plus oil respectively); (II) emission spectra ($\lambda_{\text{exc}} = 562$ nm) of PB16 in painting mock-up samples on canvas (powder plus oil); (III) emission spectra ($\lambda_{\text{exc}} = 435$ nm) of cadmium yellow PY35 (black line), orange PO20 (grey line) and red PR108 (dashed line) in painting mock-up samples on canvas (commercial oil paints). *= spurious band due to the dichroic filter.

Fig. 6. (I) Emission spectra of a painting sample with acrylic binder of the mixture PY139+PR122 ($\lambda_{\text{exc}} = 435$ nm), before (a) and after (b) correction for self-absorption. For comparison, also the corrected spectra of the two pigments (c, d) are shown; (II) Emission spectra of a painting sample with acrylic binder of the mixture PY139+PV23 ($\lambda_{\text{exc}} = 435$ nm), before (a) and after (b) correction for self-absorption. For comparison, also the corrected spectrum of PY139 is shown (c).

Fig. 7. Measurement areas and emission spectra obtained on the painting “Addetta a Zoate” (G. Faraone, 2011). (I) emission spectrum ($\lambda_{\text{exc}} = 435$ nm) of point 1 (red); (II) emission spectrum ($\lambda_{\text{exc}} = 435$ nm) of (a) point 3 (pink) after self-absorption correction, compared with that of the recognised reference pigments PO43 (b); (III) emission spectrum ($\lambda_{\text{exc}} = 435$ nm) of (a) PY35 compared with that of (b) point 4 (light green); (IV) emission spectrum ($\lambda_{\text{exc}} = 562$ nm) of (a) PV23 compared with that of (b) point 7 (violet). * = band due to oil binder.